34th Annual International Conference of the IEEE EMBS
San Diego, California USA, 28 August - 1 September, 2012

New Software Tools for Enhanced Precision in Robot-Assisted Laser Phonomicrosurgery

Giulio Dagnino, Leonardo S. Mattos, and Darwin G. Caldwell

Abstract— **This paper describes a new software package created to enhance precision during robot-assisted laser phonomicrosurgery procedures. The new software is composed of three tools for camera calibration, automatic tumor segmentation, and laser tracking. These were designed and developed to improve the outcome of this demanding microsurgical technique, and were tested herein to produce quantitative performance data. The experimental setup was based on the motorized laser micromanipulator created by Istituto Italiano di Tecnologia and the experimental protocols followed are fully described in this paper. The results show the new tools are robust and effective: The camera calibration tool reduced residual errors (RMSE) to 0.009 ± 0.002 mm under 40x microscope magnification; the automatic tumor segmentation tool resulted in deep lesion segmentations comparable to manual segmentations (RMSE = 0.160 ± 0.028 mm under 40x magnification); and the laser tracker tool proved to be reliable even during cutting procedures (RMSE = 0.073 ± 0.023 mm under 40x magnification). These results demonstrate the new software package can provide excellent improvements to the previous microsurgical system, leading to important enhancements in surgical outcome.**

I. Introduction

Laser phonomicrosurgery is a demanding surgical technique that involves the larynx and requires significant psychomotor skills [1], [2]. Currently, a major elective technology used in phonomicrosurgery is the CO_2 surgical laser coupled with the surgical microscope. In this case, the laser beam is manually aimed by means of a mechanical micromanipulator and the standard operating distance is 400 mm [3]. However, this kind of manipulation is prone to error resulting from ergonomics and inexperience factors [2].

Due to the small size of vocal cords and to the fact that lesions can be smaller than 1 mm [1], it is clear that accurate laser aiming is absolutely important in order to minimize the surgical impact on voice quality and to guarantee total pathology removal [4]. Achieving these two goals is a major challenge for the surgeons, both due to the surgical precision required and to the surgeon's ability to differentiate tumor from normal tissue. In fact, tumor identification is still based on subjective criteria that are not easily quantifiable. The development of technology to objectively assess tumor margins intraoperatively would be of great value [5].

The issues above have lead researchers both from academia and industry to focus on new technology for this field. An example is the commercial *AcuBlade* laryngeal microsurgery system (Lumenis Ltd).

Other examples include the work of Giallo, who proposed a joystick-controlled surgical system that provided the motorization of a traditional micromanipulator [2], and research on the use of the daVinci robot (Intuitive Surgical Inc.) for laser laryngeal surgeries [6].

On the side of tumor margins assessment, Nguyen *et al.* developed a method to visualize tumors during surgery using activatable cell-penetrating peptides. In this case, intraoperative real-time fluorescence imaging can be used to delineate tumor margins, resulting in improved precision of tumor resection [5].

In addition, Peretti *et al.* reported on the Narrow-Band Imaging (NBI) technique in the assessment of laryngeal cancer: NBI is an optical technique in which filtered light is used to highlight superficial carcinomas based of their neoangiogenic pattern [7].

Research towards improving laser phonomicrosurgeries is also being conducted at the Istituto Italiano di Tecnologia (IIT), and has already resulted in the development of a new computer-assisted laser phonomicrosurgery system (Fig. 1) [8]. This system has demonstrated to be more precise and offer better ergonomics than a traditional laser micromanipulator, in particular when the "virtual scalpel" control is used [9], [10].

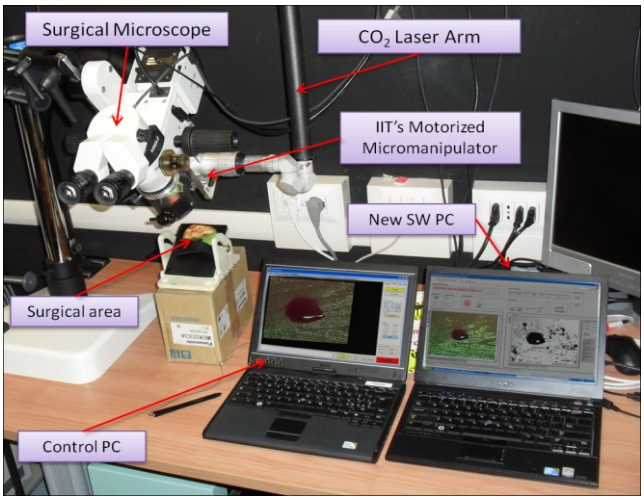

Fig. 1. The system used for robot-assisted laser phonomicrosurgery: CO_2 laser coupled with surgical microscope, the motorized micromanipulator, the control PC and the second PC on which the new software for camera calibration, tumor segmentation and laser tracking was developed and tested.

Manuscript received March 15, 2012.

G. Dagnino is with the Department of Advanced Robotics, Istituto Italiano di Tecnologia, Via Morego 30, 16163 Genova, Italy (corresponding author: phone: +39-010-71781213; fax: +39-010-720321; e-mail: giulio.dagnino@iit.it).

L. S. Mattos, and D. G. Caldwell are with the Department of Advanced Robotics, Istituto Italiano di Tecnologia, Via Morego 30, 16163 Genoa, Italy (e-mail: leonardo.dematos@iit.it, darwin.caldwell@iit.it).

In this paper we introduce and evaluate a new software created to improve laser phonomicrosurgery procedures by offering new tools for precise tumor margin detection and enhanced laser aiming control. These goals were achieved through a camera calibration and image correction tool; a laser tracking tool for laser visual servoing; and a tumor segmentation tool.

This paper starts with descriptions of the new software tools and of the experimental protocols followed to validate them. This is followed by an introduction to the data analysis methods used, and then by experimental results. Finally, the results are discussed.

II. System Description

The software tools introduced and evaluated in here are based on the laser system developed at the IIT (Fig. 1). This system includes: a CO_2 surgical laser (Opmilas CO_2 25, Zeiss), the IIT's motorized mechanical micromanipulator described in [8], one stereo surgical microscope with built-in CCD camera (Leica M651), and one tablet PC (Dell Latitude XT2). The master system controller runs on this tablet PC, which controls the laser micromanipulator.

The new software tools currently run on a second computer (Dell Latitude E4300) for development and testing purposes. The new software package is composed of three tools dedicated to 1) camera calibration, 2) tumor segmentation, and 3) laser tracking. This system has been developed using LabView 11 (National Instruments Corp.) and the NI Vision Toolkit. It works both in real-time (using video captured by a connected camera, with a resolution of 640x480 pixels) and off-line (using recorded video). In addition, the software provides a graphical user interface (GUI) that allows full control of all vision system parameters. The developed software also includes a Matlab code created to compute the root mean squared error (RMSE) on laser trajectory following tasks (i.e. laser following the edges of a segmented tumor), the maximum error observed, and graphs the obtained results. The method used to calculate the RMSE and the maximum error has been well described in [9],[10].

A. Camera Calibration

Perspective errors and lens aberration cause images to appear distorted. This distortion misplaces information in an image. In order to compensate for perspective errors and nonlinear lens distortion, calibration of the imaging system is needed. The implemented camera calibration tool consists of three steps: *1) Calibration template definition:* a grid of circular dots was used here. This grid has a known, constant displacement in the x and y directions ($dx = dy$). *2)Reference coordinate system definition:* to express measurements in real world units, a coordinate system in the image of the grid was defined by its origin, angle and axis direction. The origin (in pixels) defines the center of the coordinate system; the angle specifies its orientation with respect to the angle of the topmost row of dots in the grid image. *3) Learn the calibration information:* after the calibration grid and reference axes have been defined, images of the grid were acquired. A total of 8 pictures of the grid place in different angles were recorded for each microscope magnification (6x, 10x, 16x, 25x, 40x). Then, the "Distortion Model" calibration algorithm (NI Vision Toolkit) [11] was applied in order to compute the radial distortion introduced by the microscope lens, and to determine the conversions from pixel to real-world units (mm). This procedure was applied to all sets of images (i.e., for each microscope magnification) and calibration information was stored in five different files.

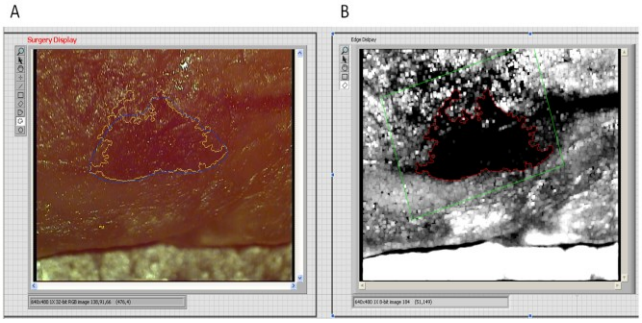

Fig. 2. Edge detection precision experiments: (A) simulation of a deep lesion by means of blood injected in chicken tissue, segmented by hand (blue line) and by edge detector (yellow line); (B) the same simulated lesion filtered and segmented (red line) by edge detector algorithm. The green square is the ROI defined by user for the automated edge detection algorithm. Microscope magnification is 40x.

Once the setup was calibrated through this procedure, the distortion models were used to automatically correct images from the microscope video streaming (or recorded video), allowing their use for precise operation using real-world units. An error statistic of the camera calibration process is presented and discussed in the section III.

B. Tumor Segmentation

This tool is based on a custom edge detection algorithm, which performs the following four steps: *1)Preparation of the image to the filtering steps:* applies a brightness, contrast and gamma correction to each color plane; *2)First filtering step:* this step extracts a single plane from the color image. The user can choose to extract one of the following planes: red, green, blue, hue, saturation, luminance, value, intensity. In this work the green extraction plane was used. The output image is a grayscale image. *3)Second filtering step:* performs grayscale morphological transformation on the image. The user can choose from the following morphological transformations: auto median, erosion, dilatation, closing, opening. Here, one iteration of the opening operation (erosion followed by a dilatation) using a 3x3 structuring element was used to remove isolated bright pixels and to smooth surfaces. This operation helps to reduce image noise and ensures the tumor margins are not underrated. *4)Contour extraction:* the contour from the input image is extracted based on a gradient filter and on the following properties: extraction mode (normal, uniform regions), edge threshold, edge filter size (fine, normal, contour tracing), minimum length of the smallest curve as described in [11].The user has to define the region of interest (ROI) in which to search for contour: the algorithm looks at the contour closest to (within) this ROI (Fig. 2.B).

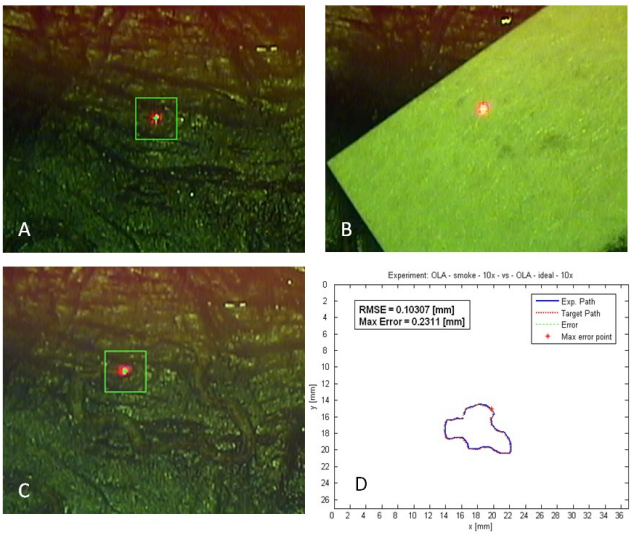

Fig. 3. Laser tracker precision experiments. Snapshots from the video recorded: (A) real condition (CO_2 off); (B) ideal condition; (C) real condition (CO_2 on, laser cutting path is visible); and (D) plot of data analysis obtained comparing the laser path in real condition (CO_2 on) and ideal condition. Microscope magnification is 10x.

C. Laser Tracker

Knowing the exactly position of the laser spot in the video frame is very important in this application. This is useful for the robotic system calibration, i.e., to compute the transformation from robot space to real-world, and also for precise laser aiming control on the surgery field via laser visual servoing.

The developed laser tracking tool consists of four steps: *1)Filtering step:* similarly to the first filtering step of the tumor segmentation tool, this filter extracts the red plane (since the laser spot is red). Then, a convolution linear filter is applied to smooth the grayscale image created (3x3 Gaussian kernel). *2)Image correction:* applies a brightness, contrast and gamma correction to the chosen color plane. *3)Template definition:* creates a description of the template that will be used during the search phase of the algorithm. This template descriptor is a copy of an area of the input image including the laser spot. This area is defined by the user. *4)Pattern matching algorithm:* during the search phase, the template descriptor is used to search for laser spot via pattern matching within the video frame (cross correlation method) [11]. The extracted coordinates of the center of the template descriptor represent the laser spot position in the video frame.

TABLE I. RESIDUAL CAMERA CALIBRATION ERRORS

Magnification	Image	Average RMSE [mm]	Average Max. Error [mm]
6x	*Calib. Template*	0.134 ± 0.078	0.153 ± 0.085
	Test Image	0.139 ± 0.091	0.156 ± 0.102
10x	*Calib. Template*	0.052 ± 0.028	0.060 ± 0.022
	Test Image	0.040 ± 0.023	0.050 ± 0.035
16x	*Calib. Template*	0.035 ± 0.012	0.047 ± 0.017
	Test Image	0.018 ± 0.008	0.027 ± 0.013
25x	*Calib. Template*	0.018 ± 0.005	0.023 ± 0.007
	Test Image	0.009 ± 0.005	0.010 ± 0.006
40x	*Calib. Template*	0.017 ± 0.006	0.026 ± 0.010
	Test Image	0.009 ± 0.002	0.012 ± 0.001

III. EXPERIMENTAL VALIDATION

The new software tools were assessed by a series of experiments designed to evaluate their accuracy. The metrics used were the RMSE between experimental and target data sets, and the maximum error observed.

A. Validation of the camera calibration tool

This tool provides a function that returns the residual error associated with the calibration template image, which was used here as a reference to evaluate distortion errors measured on test images. In this case, video streaming from the microscope camera was used to acquire the test images.

For these experiments, five images of a known circle (diameter = 5 mm, line width ≈ 0.1 mm) were acquired for each microscope magnification level, for a total of 25 images. These images were processed as follows: 1) the image was loaded in the software and corrected with the calibration parameters; 2) the user manually drew a circle exactly over the circle displayed, creating a data set that represented the experimental data; 3) a circle of 5 mm diameter, centered exactly over the center of the circle drawn by the user, was automatically generated. This represented the target data; 4) the Matlab code was used to calculate the RMSE and maximum error between experimental and target data. The good matching between the ideal (target) and the corrected images, proves the efficiency of the correction algorithm and reliability of the residual errors measurements. These results are shown in Table I.

B. Validation of the tumor segmentation tool

A slice of chicken tissue was used to simulate human tissue, and human blood was injected in the chicken slice to simulate a lesion (Fig. 2). A total of six simulated lesions were created: three superficial lesions, injecting blood on the surface of the test tissue; and three deep lesions injecting blood deep inside the test tissue.

Then, one picture of each simulated lesion was taken for each microscope magnification, for a total of 30 images. These images were subsequently segmented manually using a graphics tablet (Wacom CTH-670) to create the ground-truth images used for evaluating the new segmentation tool.

The test images were then segmented automatically by the developed software, and the resulting tumor contours were analyzed in terms of their RMSE and maximum error (maximum distance between the automatically defined contour and the one defined manually). Results are shown in Table II. In case of superficial lesions that are well visible and identifiable, the measured RMSE was lower than for the case of deep lesions. However, the maximum errors were quite similar and small in both cases – only 0.635 mm on average. This indicates the automatic segmentation works well and is comparable to the manual segmentation. In the case of deep lesions, the higher RMSE resulted from the user's difficulty to identify the lesion bounds in the surgery display. However, the same image filtered by the tumor detector make the deep lesion appear clearly separated from the background (i.e. healthy tissue), facilitating the identification of its edge (Fig. 2.B). This is an interesting and useful result for automatic tumor detection as well as for manual tumor segmentation.

TABLE II. TUMOR SEGMENTATION EXPERIMENTS: RESULTS

Magnification	Lesion	Average RMSE [mm]	Average Max. Error [mm]
6x	***Superficial***	0.196 ± 0.148	0.595 ± 0.474
	Deep	0.150 ± 0.026	0.495 ± 0.172
10x	***Superficial***	0.197 ± 0.079	0.752 ± 0.241
	Deep	0.213 ± 0.131	0.668 ± 0.523
16x	***Superficial***	0.190 ± 0.055	0.633 ± 0.089
	Deep	0.291 ± 0.164	0.833 ± 0.475
25x	***Superficial***	0.188 ± 0.003	0.612 ± 0.012
	Deep	0.254 ± 0.175	0.651 ± 0.451
40x	***Superficial***	0.175 ± 0.227	0.690 ± 0.871
	Deep	0.160 ± 0.028	0.508 ± 0.159

TABLE III. LASER TRACKER EXPERIMENTS: RESULTS

Magnification	Condition	Average RMSE [mm]	Average Max. Error [mm]
6x	***R vs I***	0.109 ± 0.022	0.249 ± 0.040
	RCO_2 vs I	0.108 ± 0.017	0.244 ± 0.082
10x	***R vs I***	0.080 ± 0.014	0.219 ± 0.013
	RCO_2 vs I	0.082 ± 0.019	0.193 ± 0.064
16x	***R vs I***	0.105 ± 0.024	0.430 ± 0.138
	RCO_2 vs I	0.134 ± 0.012	0.397 ± 0.131
25x	***R vs I***	0.073 ± 0.025	0.164 ± 0.028
	RCO_2 vs I	0.106 ± 0.018	0.198 ± 0.050
40x	***R vs I***	0.060 ± 0.031	0.124 ± 0.048
	RCO_2 vs I	0.073 ± 0.023	0.138 ± 0.040

R = real condition (CO_2 off); RCO_2 = real condition (CO_2 on); I = ideal condition

C. *Validation of the laser tracker tool*

Three series of experiments were performed; each of them consisting in recording video of the laser moving in the surgical field along a preset path. A different path was defined and used for each experimental series. Video of the laser was recorded in three different conditions: *1)Real condition (CO_2 off):* the laser was aimed along the preset path on a chicken slice injected with blood to simulate lesions. The laser spot was tracked without cutting or ablating (Fig. 3.A). *2)Real condition (CO_2 on):* as the condition above, but with the CO_2 laser beam on. In this case, the tested tissue was cut and surgical smoke was produced (Fig. 3.C). *3)Ideal condition:* the chicken slice was masked with a piece of yellow paper on which the red laser spot was clearly visible and trackable. Also in this case the CO_2 laser was off (Fig. 3.B). For each experimental condition described above, one video was recorded for each microscope magnification, therefore resulting in a total of 45 videos. Laser tracking results from these videos were then analyzed and compared with the paths extracted from the ideal conditions, providing the performance metrics shown in Table III and depicted in Fig. 3.D. The evaluation results show the laser tracker is very precise also during cutting procedures: the tracker tool never lost the laser spot, even when it passed over the lesions or when tissue was cut producing surgical smoke.

IV. CONCLUSION

This paper presented a novel software package created to improve the precision and safety of robot-assisted laser phonomicrosurgeries. The entire system was described herein and evaluation experiments were presented.

The camera calibration tool demonstrate to efficient image correction, providing a residual RMSE of only 0.009 ± 0.002 mm at the higher microscope magnification (40x) over a 5 mm diameter circular target. This indicates the calibration tool is a solid basis for other processing and control systems based on the microscope images.

Validation trials with the tumor detector tool highlighted an interesting aspect: it is very difficult to perform deep lesions segmentation using white light. The developed algorithm provided a filtering section that facilitates both automatic lesion segmentation and manual segmentation by the system's user. This is highly valuable and important for the outcome of surgeries, and has great potential to serve as a real-time assistive tool for improving surgical outcome. Furthermore, the results from automatic segmentation of deep lesions (average RMSE of 0.160 ± 0.028 mm at 40x) were demonstrated comparable to manual segmentation, showing that the developed tumor detector is a suitable and useful tool to help surgeons. Further studies will validate the proposed tumor segmentation tool using images of real tumors and more accurate detection techniques like NBI.

Finally, the laser tracker tool was demonstrated robust and reliable, successfully tracking the laser spot at camera frame rate (30 fps) even during laser cutting procedures. In these cases an average tracking RMSE of 0.073 ± 0.023 mm was measured (in real condition at 40x).

ACKNOWLEDGMENT

The research has received funding from the European Union Seventh Framework Programme FP7/2007-2013 – Challenge 2 – Cognitive Systems, Interaction, Robotics – under grant agreement µRALP - n°288233.

REFERENCES

[1] S. M. Zeitels. Atlas of phonomicrosurgery and other endolaryngeal procedures for benign and malignant disease. San Diego, CA: Singular, 2001.

[2] J. F. Giallo. A Medical Robotic System for Laser Phonomicrosurgery. *PhD Dissertation, North Carolina State University*, 2008.

[3] M. Remacle, V. Oswal. Principles and practice of lasers in otolaryngology and head and neck surgery. Kugler Publications, The Hague, The Netherlands, 2002.

[4] S. Chawla and A. S. Carney, "Organ preservation surgery for laryngeal cancer", *Head & Neck Oncology*, 1:12, May 2009.

[5] Q. T. Nguyen, R. Y. Tsien et al. "Surgery with molecular fluorescence imaging using activable cell-penetrating peptides decreases residual cancer and improves survival", *PNAS,* 2010, vol. 107, n°9.

[6] C. A. Solares and M. Strome, "Robot-Assisted CO2 Laser Supraglottic Laryngectomy: Experimental and Clinical Data" *Laryngoscope* vol. 117(5):817-820, May 2007.

[7] G. Peretti et al. "Narrow-band imaging: a new tool for evaluation of head and neck squamous cell carcinomas. Review of the literature", *Acta Otorhinolaryngol Ital* 2008; 28:49-54.

[8] L. S. Mattos, M. Dellepiane, and D. G. Caldwell, "Next-Generation Micromanipulator for Computer-Assisted Laser Phonomicrosurgery", EMBC 2011, Boston, MA, USA.

[9] G. Dagnino, L. S. Mattos, G. Becattini, M. Dellepiane, and D. G. Caldwell, "Comparative evaluation of user interfaces for robot-assisted laser phonomicrosurgery", EMBC 2011, Boston, MA, USA.

[10] L. S. Mattos, G. Dagnino, G. Becattini, M. Dellepiane, and D. G. Caldwell, "A virtual scalpel system for computer-assisted laser miscrosurgery", IROS 2011, San Francisco, CA, USA.

[11] "Imaq Vision Concepts Manual", available from: http://www.ni.com/pdf/manuals/322916b.pdf